

10.1071/CH14024\_AC

©CSIRO 2015

Australian Journal of Chemistry 2015, 68(3), 471-480

## SUPPLEMENTARY MATERIAL

### **Investigation of the photodegradation of Reactive Blue 19 on P-25 titanium dioxide: effect of experimental parameters**

*Faridah Abu Bakar<sup>A,B</sup>, Jan-Yves Ruzicka<sup>A</sup>, Ida Nuramdhani<sup>C</sup>, Bryce E. Williamson<sup>A</sup>, Meike Holzenkaempfer<sup>A</sup>, and Vladimir B. Golovko<sup>A,D,E</sup>*

<sup>A</sup> Department of Chemistry, University of Canterbury, Private Bag 4800, Christchurch 8140, New Zealand

<sup>B</sup> Universiti Tun Hussein Onn Malaysia, 86400 Parit Raja, Batu Pahat, Johor, Malaysia

<sup>C</sup> Sekolah Tinggi Teknologi Tekstil, Bandung, Indonesia

<sup>D</sup> The MacDiarmid Institute for Advanced Materials and Nanotechnology

<sup>E</sup> Corresponding author. Email: [vladimir.golovko@canterbury.ac.nz](mailto:vladimir.golovko@canterbury.ac.nz)

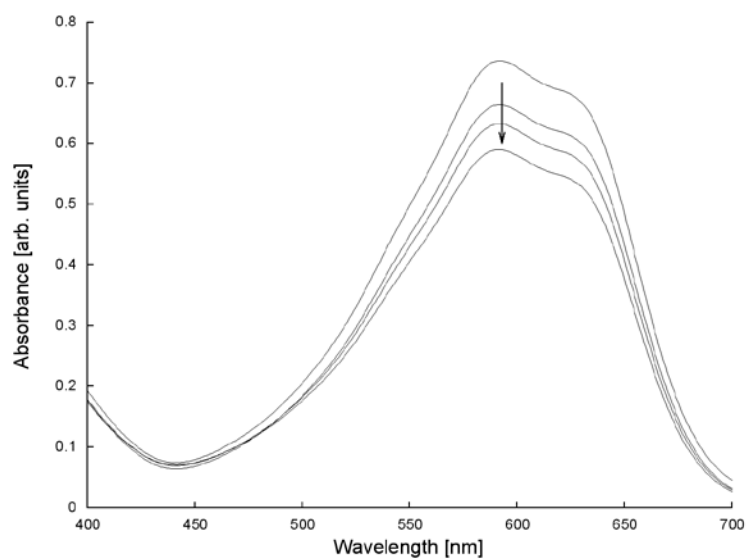


**Figure S1:** UV-vis absorption spectrum of RB-19. Photodegradation causes a decrease in concentration, monitored as a decrease in the magnitude of absorbance at  $\lambda = 593$  nm (shown by the arrow).

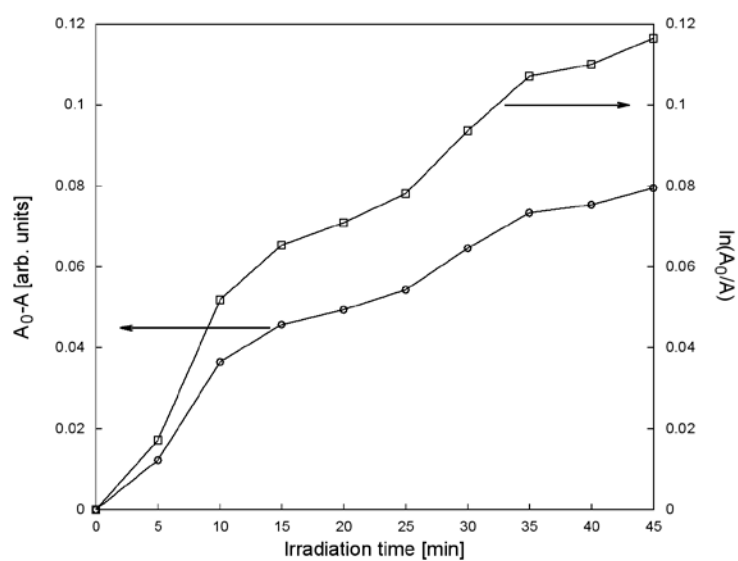


**Figure S2:** Zero- (left-hand ordinate) and first-order (right-hand ordinate) kinetic plots for the degradation of RB-19 on titanium dioxide.

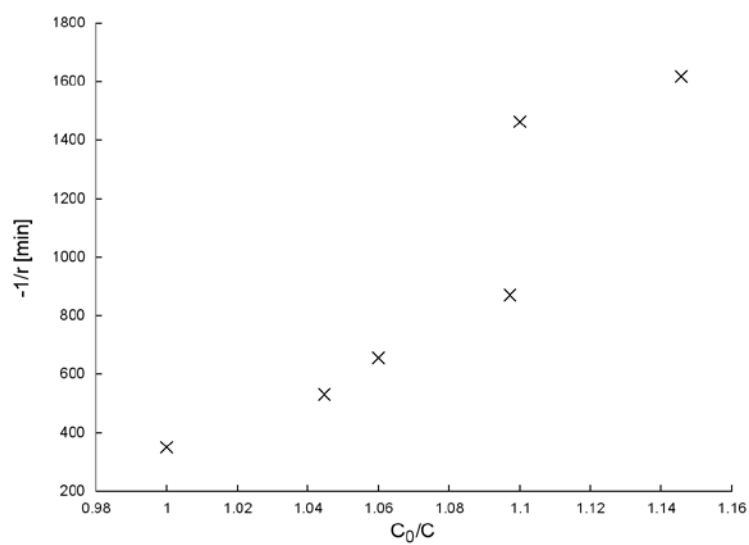


**Figure S3:** Attempted Langmuir-Hinshelwood fitting of a typical photodegradation experiment (here: buffered at pH 7 using  $\text{KH}_2\text{PO}_4/\text{NaOH}$ ).

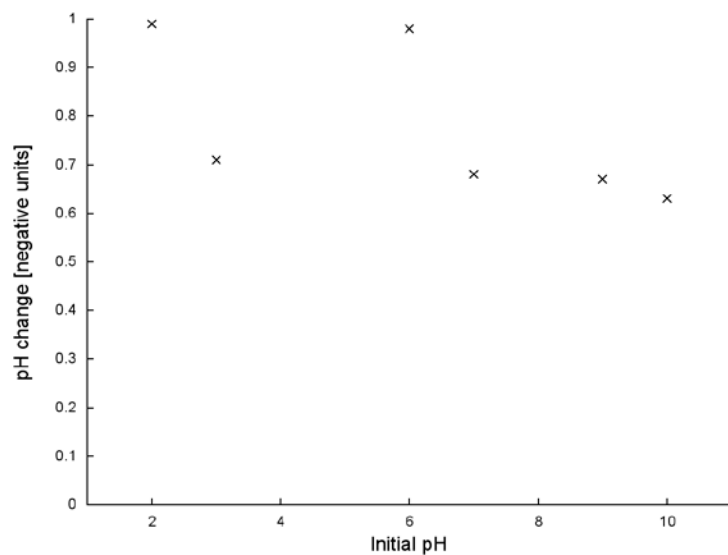


**Figure S4:** pH change of RB-19-titania systems after 120 minutes of irradiation.

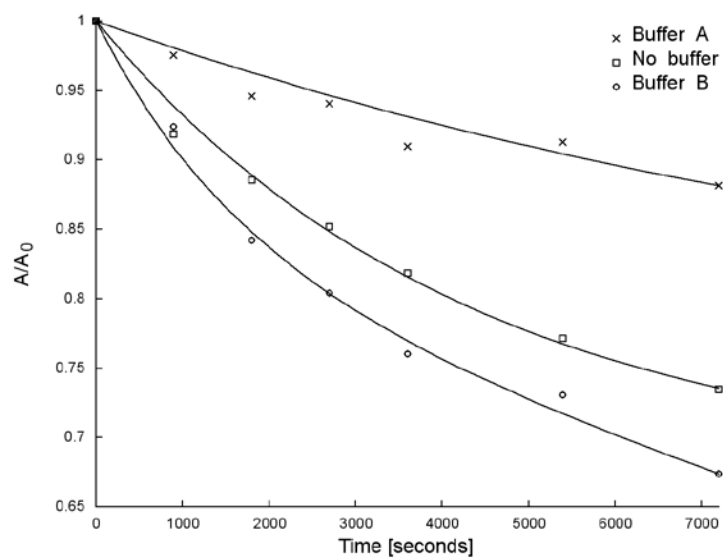
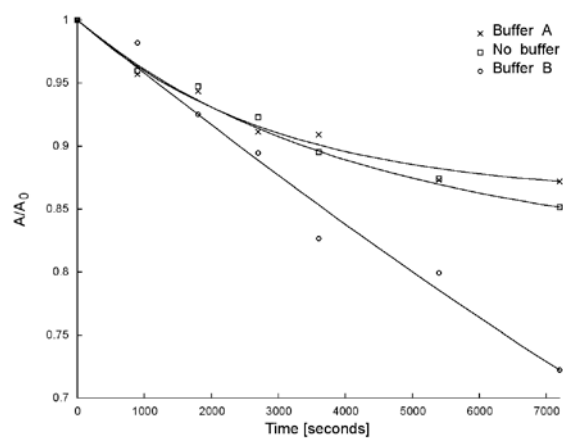
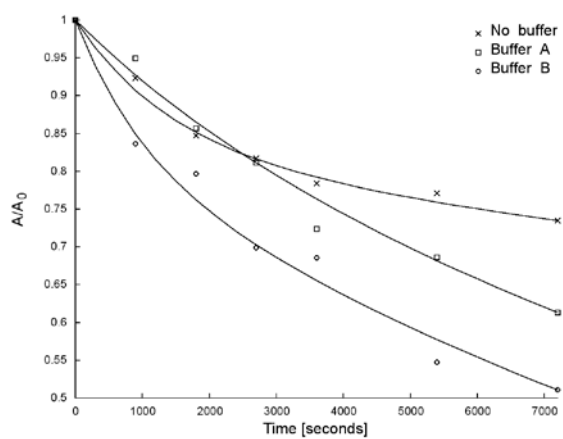


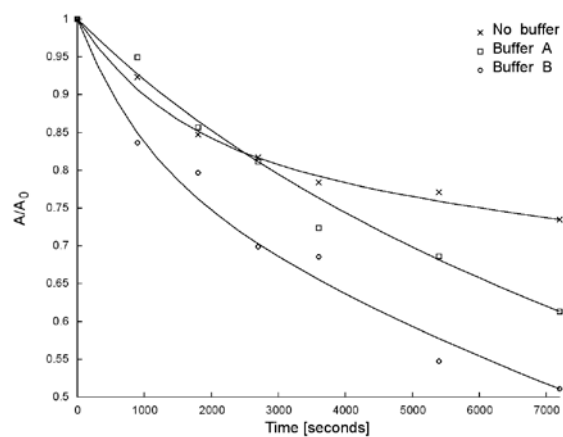
**Figure S5:** Extent of photodegradation of RB-19 on  $\text{TiO}_2$  at various pHs. In-series first-order fitting is shown as solid lines.



**a. pH 3**



**b. pH 7**



**c. pH 10**

**Figure S6:** Extent of photodegradation of RB-19 on  $\text{TiO}_2$  using buffers. In-series first-order fitting is shown as solid lines.

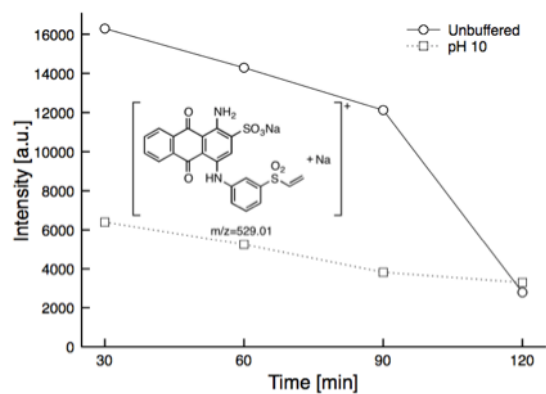


Figure S7: Uniblu A photodegradation product as detected by mass spectrometry.

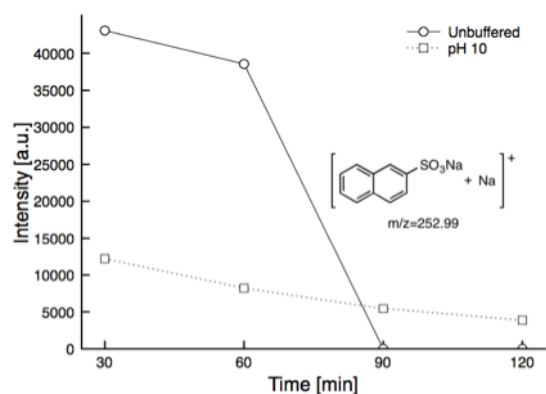
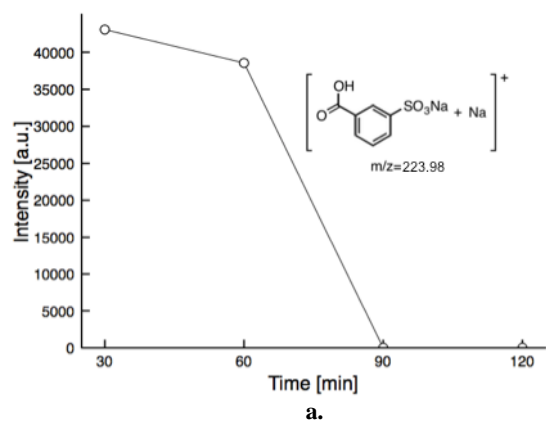
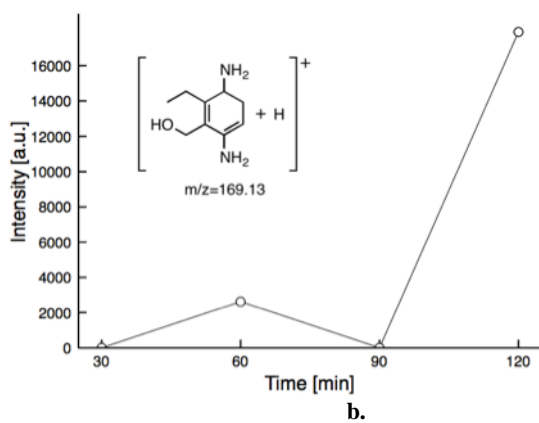


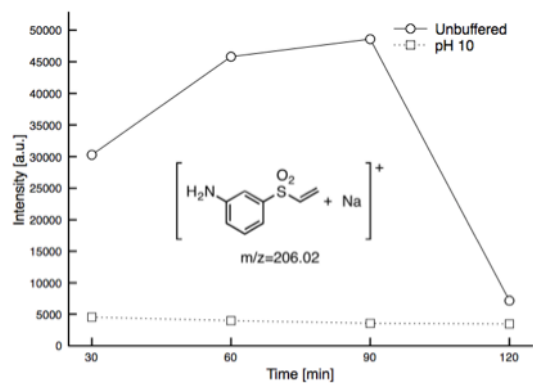
Figure S8: Photodegradation of sodium naphthalene sulfonate over time, as detected by mass spectrometry.



a.



b.



c.

**Figure S9:** Photodegradation products containing the benzene moiety over time, as detected by mass spectrometry.

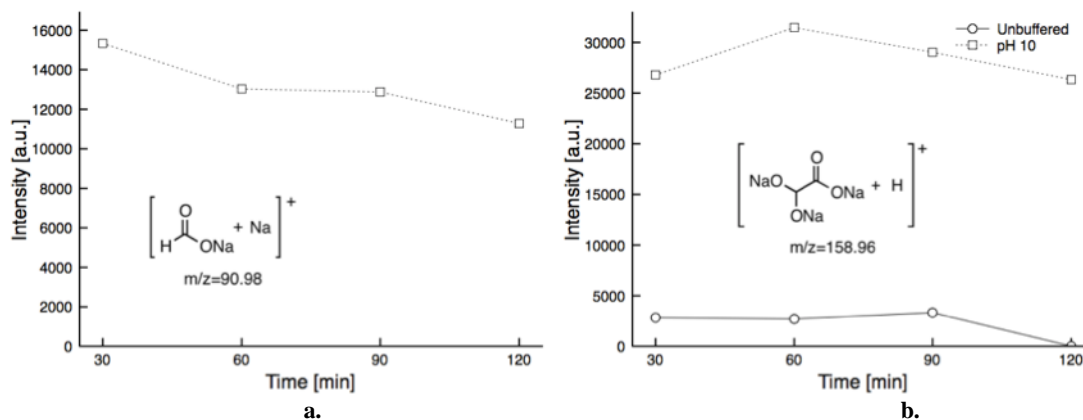
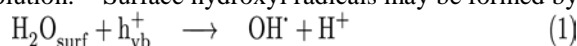


**Figure 10:** Small photodegradation products over time, as detected by mass spectrometry.

## 1. Discussion on indirect photodegradation pathways

Indirect photodegradation occurs via the production of hydroxyl radicals, which then attack the dye in solution.<sup>1,2</sup> Surface hydroxyl radicals may be formed by one of two reactions:



Equation 1 is independent of pH, and accounts for hydroxyl production in both acidic and basic media. Equation 2, however, depends on the concentration of hydroxide ions near the catalyst surface, and thus proceeds more efficiently in basic solution.

## 2. Discussion of MS results

The relative signal of Uniblue A (UBA), the sole anthraquinone derivative detected by MS, is shown in Figure S7. This intermediate dye is formed by the elimination of sulfuric acid (see Scheme 1, main article). Despite a strong argument that UBA should be more prevalent in basic solution, an appreciably higher concentration is observed for the unbuffered solution. It may be that UBA is more readily decomposed under basic conditions, and that by the time MS measurement started, the majority of UBA had already been degraded to give smaller products.

The relative signal of sodium naphthalene sulfonate (SNS), the one photodegradation intermediate containing the naphthalene moiety, is shown in Figure S8. SNS appears in solution in both unbuffered and buffered systems after only thirty minutes of irradiation, and slowly disappears over time, suggesting gradual degradation to less complex products. It is observed that degradation accelerates after ninety minutes.

The concentration of the three intermediates containing the benzene moiety is shown in Figure S9. Each displays considerably different behavior in solution, however all exist in much higher concentration in the unbuffered system. While this may be a result of differing degradation pathways, it may also be because they are rapidly degraded in basic solution due to hydroxyl radical attack.

The vinylsulfonyl aniline (VSA) molecule (Figure S9a) could easily be produced by the cleavage of the N-C bond marked A in Figure 5, main article, followed (or preceded) by vinyl sulfone formation (Scheme 1, main article). The concentration of diamino-ethylcyclohexadienyl methanol (Figure S9b) remains low or zero for the initial ninety minutes of the reaction, but increases sharply past this point. This suggests that at some point between ninety and 120 minutes, a larger, more complex intermediate starts to break down, giving rise to a

variety of products (see also the degradation of sodium naphthalene sulfonate above). In contrast, sodium carboxycyclohexane sulfonate (Figure S9c) is present in high concentration after only thirty minutes, but its concentration quickly drops after this until after ninety minutes it is completely degraded. This intermediate is most likely formed by the breakdown of the anthraquinone moiety of the RB-19 dye.

The relative concentration of smaller degradation intermediates appearing in solution over the course of the reaction is shown in Figure S10. Just two of these could be reliably detected over the course of the entire reaction, and neither could be attributed to any definitive structural origin within the RB-19 dye. Both appeared in much higher concentration in the basic system. This is likely due to the enhanced activity of this system, and may be also be a result of the indirect photodegradation pathway.

## References

1. M. Muruganandham. *Dyes and Pigments*, 2006, 68, 133–142.
2. F. Herrera, A. Lopez, G. Mascolo, P. Albers, J. Kiwi. *Water Research*, 2001, 35, 750–760.